

Phase diagrams of the generalized spin- $\frac{1}{2}$ ladder under staggered field and dimerization: A renormalization group study

Y.-J. Wang

Max-Planck-Institut für Physik Komplexer Systeme, Nöthnitzer Straße 38, 01187 Dresden, Germany

(Dated: November 16, 2018)

In the weak-coupling regime of the continuous theories, two sets of one-loop renormalization group equations are derived and solved to disclose the phase diagrams of the antiferromagnetic generalized two-leg spin- $\frac{1}{2}$ ladder under the effect of (I) a staggered external magnetic field and (II) an explicit dimerization. In model (I), the splitting of the $SU(2)_2$ critical line into $U(1)$ and Z_2 critical surfaces is observed; while in model (II), two critical surfaces arising from their underlying critical lines with $SU(2)_2$ and Z_2 characteristics merge into an $SU(2)_1$ critical surface on the line where the model attains its highest symmetry.

PACS numbers: 75.10.Jm, 71.10.Pm, 64.60.Ak, 05.70.Jk

I. INTRODUCTION

The physics of quantum phase transitions in one-dimensional systems has attracted much attention in recent years because not only of its speciality—the conformal symmetries and universalities in (1+1)-critical models,^{1,2,3} but also of its generality—the quantum critical phenomena in higher dimensions.⁴ A general question is posed as follows: If a critical system defined in the ultraviolet limit is deformed by more than one relevant perturbations, what is the fate of the system? Can the criticality be reached again in the infrared limit because of the “cancellation” effect among these perturbations, thus a quantum phase transition takes place? A typical model of this sort is the so-called double-frequency sine-Gordon model,^{5,6} where an Ising transition was thought to be driven by two competing relevant perturbations. The description of the phase transition requires a non-perturbative scheme being able to identify correctly those degrees of freedom that remain massive and the low-energy ones that eventually become critical and undergo the transition.

The same strategy was extended to a more complicated non-Abelian case—a two-leg spin- $\frac{1}{2}$ Heisenberg antiferromagnetic ladder subject to a site-parity-breaking dimerization field.⁷ The non-trivial aspect of the non-perturbative approach adopted in this study of the strong-coupling limit of the model is that one has to preserve the $SU(2)$ symmetry, which cannot be spontaneously broken, in the Ising model language which apparently has only a discrete symmetry. This hidden symmetry was realized when using very non-local duality transformations for the coupled Ising models. An effective low-energy Hamiltonian depicting the ensuing quantum phase transition was derived and the transmutation of all physical fields at the infrared fixed point was identified. It was unambiguously shown that a quantum phase transition occurs from the universality class of $SU(2)$ level 2 Wess-Zumino-Novikov-Witten (WZNW) model in the ultraviolet limit to the universality class of $SU(2)$ level 1 WZNW model in the infrared limit.

Another possible scenario was set up by introducing a staggered magnetic field, which explicitly breaks both $SU(2)$ and bond-parity symmetries, to the generalized spin ladder.⁸ Depending on which phase the model belongs to in absence of the staggered field, either $U(1)$ or Z_2 criticality was predicted under the effect of the staggered field. An interesting new phase that interpolates between the Haldane spin liquid phase and the spontaneously dimerized phase was found beyond the transitions. The main features of this intermediate phase are: partially (transverse) coherent spin excitations and partially (longitudinal) non-vanishing string order parameter.

As we can see, the physics of the generalized spin- $\frac{1}{2}$ ladder under the effect of the dimerization or the staggered field is very rich. In this paper, we shall scrutinize these two models in a more general perspective and try to understand the phase diagrams as a whole. Our main attention is to be paid to the overall topology of the phase diagrams; while the physical properties in various phases are only to be mentioned briefly if available.

The paper is organized as follows. In Sec. II, we present a short overview of the continuous version of our models. In Sec. III, we derive two sets of renormalization group (RG) equations and central charge formulas. These equations are (numerically) solved and analyzed in Sec. IV to bring about the phase diagrams of the continuous models. The implication to the ladder systems is summarized and concluded in Sec. V.

II. MODELS AND THEIR CONTINUOUS FIELD-THEORETIC MAPPINGS

We consider a standard two-leg spin- $\frac{1}{2}$ antiferromagnetic ($J > 0$) Heisenberg ladder (J_\perp) generalized to include a four-spin interaction (V):^{9,10}

$$H_{\text{gen}} = J \sum_{a=1,2} \sum_n \mathbf{S}_{a,n} \cdot \mathbf{S}_{a,n+1} + J_\perp \sum_n \mathbf{S}_{1,n} \cdot \mathbf{S}_{2,n} + V \sum_n (\mathbf{S}_{1,n} \cdot \mathbf{S}_{1,n+1})(\mathbf{S}_{2,n} \cdot \mathbf{S}_{2,n+1}), \quad (1)$$

superimposed by either a staggered magnetic field, model (I),

$$H_h = h \sum_{a=1,2} \sum_n (-1)^n S_{a,n}^z, \quad (2)$$

or a π -phase (relative) dimerization, model (II),

$$H_\Delta = \Delta \sum_{a=1,2} \sum_n (-1)^{n+a} \mathbf{S}_{a,n} \cdot \mathbf{S}_{a,n+1}. \quad (3)$$

Throughout the paper, we treat the models only in the weak-coupling regime, providing

$$|J_\perp|, |V|, |h| \text{ (or } |\Delta|) \ll J. \quad (4)$$

In this limit, the field-theoretic approach in continuum is of advance and power in describing the low-energy physics of the models. In fact, the resulting Hamiltonians are represented by four interacting Majorana (real) fermions or, equivalently, four coupled Ising models.

According to Refs. 7,8,9,11, we have the following mappings in terms of Majoranas ($\xi_{R,L}$) and Ising variables (σ, μ):

$$\mathcal{H}_{\text{gen}} = \mathcal{H}_{\text{crit}} + \mathcal{H}_{\text{mass}} + \mathcal{H}_{\text{marg}}, \quad (5)$$

where the critical theory

$$\mathcal{H}_{\text{crit}} = -\frac{iv}{2} \sum_{\mu=0}^3 (\xi_R^\mu \partial_x \xi_R^\mu - \xi_L^\mu \partial_x \xi_L^\mu) \quad (6)$$

having an O(4) symmetry is inherited from two decoupled Heisenberg chains with $\text{SU}(2) \times \text{SU}(2)$ symmetry, $v \sim Ja$.¹² The mass terms result from part of the interchain coupling (J_\perp) and the four-spin interaction (V), both of which have the same scaling dimension, $d = 1$:

$$\mathcal{H}_{\text{mass}} = -im_s \xi_R^0 \xi_L^0 - im_t \boldsymbol{\xi}_R \cdot \boldsymbol{\xi}_L, \quad (7)$$

where the singlet (associated with ξ^0) and triplet ($\boldsymbol{\xi} = (\xi^1, \xi^2, \xi^3)$) masses are related to the parameters of the lattice spin model by

$$m_s = -3cJ_\perp - c'V, \quad m_t = cJ_\perp - c'V, \quad (8)$$

respectively. Here c and c' are some *positive* constants. The marginal terms are from the current-current part of the interchain coupling with scaling dimension $d = 2$:

$$\mathcal{H}_{\text{marg}} = \frac{1}{2} g_1 (\boldsymbol{\xi}_R \cdot \boldsymbol{\xi}_L)^2 + g_2 (\boldsymbol{\xi}_R \cdot \boldsymbol{\xi}_L) (\xi_R^0 \xi_L^0), \quad (9)$$

where $g_1 = \frac{1}{2} J_\perp a - \gamma$ and $g_2 = -\frac{1}{2} J_\perp a - \gamma$, with $\gamma (> 0)$ the marginally irrelevant coupling in the chains. Obviously, the symmetry of the continuous model \mathcal{H}_{gen} is $\text{O}(3) \times \text{Z}_2$, corresponding to $\text{SU}(2) \times \text{Z}_2$ for the lattice model (1) (Z_2 arising from the interchange of two chains), unless $J_\perp = 0$ when the highest symmetry of O(4) is reached, corresponding to $\text{SU}(2) \times \text{SU}(2)$.

The field-theoretic counterparts of the staggered field (2) and the dimerization (3) are represented, respectively, by

$$\mathcal{H}_h = (h/\alpha) \sigma_1 \sigma_2 \mu_3 \mu_0, \quad (10)$$

$$\mathcal{H}_\Delta = (\Delta/\alpha) \sigma_1 \sigma_2 \sigma_3 \sigma_0, \quad (11)$$

where α with a magnitude order of the lattice constant is the short-distance cut-off of the theory. While \mathcal{H}_Δ keeps the O(3) invariance for the triplet sector intact, \mathcal{H}_h breaks this symmetry down to $\text{O}(2) \times \text{Z}_2$. This is a reflection of the oriented field (2) lowers $\text{SU}(2)$ to $\text{U}(1) \times \text{Z}_2$.

In what follows, we shall address model (I): $\mathcal{H}_{\text{gen}} + \mathcal{H}_h$, and model (II): $\mathcal{H}_{\text{gen}} + \mathcal{H}_\Delta$, in RG approach. Our purpose aims at drawing the phase diagrams by analyzing the infrared properties of the RG equations.

III. DERIVATION OF THE RG EQUATIONS

It is rather straightforward to establish the one-loop RG equations out of the operator product expansions¹ (OPE's) between the perturbative operators.¹³ For a critical model perturbed by

$$\mathcal{H}_{\text{pert}} = \frac{v}{\pi\alpha^2} \sum_i \lambda_i \mathcal{O}_i, \quad (12)$$

where λ_i are dimensionless coupling constants of the corresponding dimensionless operators \mathcal{O}_i (with scaling dimension d_i), if \mathcal{O}_i are normalized in such a way that

$$\langle \mathcal{O}_i(z, \bar{z}) \mathcal{O}_j(0, 0) \rangle = \delta_{ij} \left(\frac{\alpha}{|z|} \right)^{2d_i}, \quad (13)$$

($z = v\tau + ix$ being the time-space in complex coordinates) and the short-distance OPE's satisfy

$$\mathcal{O}_i(z, \bar{z}) \mathcal{O}_j(0, 0) \sim c_{ij}^k \left(\frac{\alpha}{|z|} \right)^{d_i + d_j - d_k} \mathcal{O}_k(0, 0), \quad (14)$$

the one-loop RG equations for λ_i are readily given by

$$\dot{\lambda}_k \equiv \frac{d\lambda_k}{d \ln L} = (2 - d_k) \lambda_k - \sum_{ij} c_{ij}^k \lambda_i \lambda_j + O(\lambda^3). \quad (15)$$

In addition, the central charge satisfying Zamolodchikov's decreasing theorem¹⁴ is perturbatively evaluated to this order to be

$$C(\{\lambda\}) = C_{\text{UV}} - 3 \sum_k (2 - d_k) \lambda_k^2 + 2 \sum_{ijk} c_{ij}^k \lambda_i \lambda_j \lambda_k + O(\lambda^4), \quad (16)$$

where C_{UV} is the central charge of the unperturbed critical system (the ultraviolet fixed point). In the present case, $C_{\text{UV}} = 2$ is the central charge of two decoupled chains.

Under normalization (13), the OPE coefficients c_{ij}^k are related to the three-point function $\langle \mathcal{O}_i \mathcal{O}_j \mathcal{O}_k \rangle$, and thus are complete symmetric among the indices (ijk) .¹ Not only this procedure simplifies the calculations, but also is it essential to give rise to a correct form for the central charge (16).

A. RG equations for model (I)

Since for this model,

$$\mathcal{H}_{\text{pert}}^{(I)} = \mathcal{H}_{\text{mass}} + \mathcal{H}_{\text{marg}} + \mathcal{H}_h, \quad (17)$$

and noticing \mathcal{H}_h breaks the $O(3)$ symmetry in the triplet sector, we have to divide the triplet mass m_t and the marginal coupling constants g_1 and g_2 into doublets and singlets. Denoting the mass bilinear (or energy density) of the Ising model, $\varepsilon_\mu = i\xi_R^\mu \xi_L^\mu$, we write down:

$$\begin{aligned} \mathcal{H}_{\text{pert}}^{(I)} &= -m_t^d(\varepsilon_1 + \varepsilon_2) - m_t^s \varepsilon_3 - m_s \varepsilon_0 \\ &\quad - g_1^d \varepsilon_1 \varepsilon_2 - g_1^s(\varepsilon_1 + \varepsilon_2) \varepsilon_3 \\ &\quad - g_2^d(\varepsilon_1 + \varepsilon_2) \varepsilon_0 - g_2^s \varepsilon_3 \varepsilon_0 \\ &\quad + (h/\alpha) \sigma_1 \sigma_2 \mu_3 \mu_0 \\ &= \frac{v}{\pi \alpha^2} \sum_{i=1}^8 \lambda_i \mathcal{O}_i, \end{aligned} \quad (18)$$

where the dimensionless operators in both fermion and Abelian boson representations (“+/-” associated with sectors $(1, 2)/(3, 0)$, respectively):

$$\begin{aligned} \mathcal{O}_1 &= -\sqrt{2} \pi \alpha (\varepsilon_1 + \varepsilon_2) = -\sqrt{2} \cos \sqrt{4\pi} \Phi_+, \\ \mathcal{O}_2 &= -2\pi \alpha \varepsilon_3 = -\cos \sqrt{4\pi} \Phi_- + \cos \sqrt{4\pi} \Theta_-, \\ \mathcal{O}_3 &= -2\pi \alpha \varepsilon_0 = -\cos \sqrt{4\pi} \Phi_- - \cos \sqrt{4\pi} \Theta_-; \\ \mathcal{O}_4 &= -(2\pi \alpha)^2 \varepsilon_1 \varepsilon_2 = 4\pi \alpha^2 \bar{\partial} \Phi_+ \partial \Phi_+, \\ \mathcal{O}_5 &= -2\sqrt{2} (\pi \alpha)^2 (\varepsilon_1 + \varepsilon_2) \varepsilon_3 \\ &= -\sqrt{2} \cos \sqrt{4\pi} \Phi_+ (\cos \sqrt{4\pi} \Phi_- - \cos \sqrt{4\pi} \Theta_-), \\ \mathcal{O}_6 &= -2\sqrt{2} (\pi \alpha)^2 (\varepsilon_1 + \varepsilon_2) \varepsilon_0 \\ &= -\sqrt{2} \cos \sqrt{4\pi} \Phi_+ (\cos \sqrt{4\pi} \Phi_- + \cos \sqrt{4\pi} \Theta_-), \\ \mathcal{O}_7 &= -(2\pi \alpha)^2 \varepsilon_3 \varepsilon_0 = 4\pi \alpha^2 \bar{\partial} \Phi_- \partial \Phi_-; \\ \mathcal{O}_8 &= 2\sigma_1 \sigma_2 \mu_3 \mu_0 = 2 \sin \sqrt{\pi} \Phi_+ \cos \sqrt{\pi} \Phi_-. \end{aligned} \quad (19)$$

The scaling dimensions, $d_{1,2,3} = 1$, $d_{4,5,6,7} = 2$, and $d_8 = \frac{1}{2}$. Accordingly, the dimensionless coupling constants:

$$\begin{aligned} \lambda_1 &\equiv \frac{\eta_1}{\sqrt{2}} = \frac{m_t^d \alpha}{\sqrt{2} v}, & \lambda_2 &\equiv \frac{\eta_2}{2} = \frac{m_t^s \alpha}{2v}, \\ \lambda_3 &\equiv \frac{\eta_3}{2} = \frac{m_s \alpha}{2v}; \\ \lambda_4 &\equiv \frac{\eta_4}{4} = \frac{g_1^d}{4\pi v}, & \lambda_5 &\equiv \frac{\eta_5}{2\sqrt{2}} = \frac{g_1^s}{2\sqrt{2}\pi v}, \\ \lambda_6 &\equiv \frac{\eta_6}{2\sqrt{2}} = \frac{g_2^d}{2\sqrt{2}\pi v}, & \lambda_7 &\equiv \frac{\eta_7}{4} = \frac{g_2^s}{4\pi v}; \\ \lambda_8 &\equiv \frac{\eta_8}{2} = \frac{\pi h}{2v}. \end{aligned} \quad (20)$$

It is easy to calculate all the OPE coefficients by using either fermion or boson representation. For example, we find¹⁵

$$\begin{aligned} \mathcal{O}_8(z, \bar{z}) \mathcal{O}_8 &\sim \frac{\alpha}{|z|} + \frac{1}{\sqrt{2}} \mathcal{O}_1 - \frac{1}{2} (\mathcal{O}_2 + \mathcal{O}_3) \\ &+ \left(\frac{\alpha}{|z|} \right)^{-1} \left[\frac{1}{2\sqrt{2}} (\mathcal{O}_5 + \mathcal{O}_6) - \frac{1}{4} (\mathcal{O}_4 + \mathcal{O}_7) \right]. \end{aligned} \quad (21)$$

Therefore, we read off

$$\begin{aligned} c_{88}^1 &= \frac{1}{\sqrt{2}}, & c_{88}^2 &= c_{88}^3 = -\frac{1}{2}, \\ c_{88}^5 &= c_{88}^6 = \frac{1}{2\sqrt{2}}, & c_{88}^4 &= c_{88}^7 = -\frac{1}{4}. \end{aligned} \quad (22)$$

The algebra in this way is closed, and we list all the coefficients in Table I.

TABLE I: OPE coefficients c_{ij}^k (given in the parentheses, in front are indices k).

$i \setminus j$	1	2	3	4	5	6	7	8
1	4(-1)	5(-1)	6(-1)	1(-1)	2(-1)	3(-1)		$8(\frac{1}{\sqrt{2}})$
2	5(-1)		7(-1)		1(-1)		3(-1)	$8(-\frac{1}{2})$
3	6(-1)	7(-1)				1(-1)	2(-1)	$8(-\frac{1}{2})$
4	1(-1)				5(-1)	6(-1)		$8(-\frac{1}{4})$
5	2(-1)	1(-1)		5(-1)	4(-1)	7(-1)	6(-1)	$8(\frac{1}{2\sqrt{2}})$
6	3(-1)		1(-1)	6(-1)	7(-1)	4(-1)	5(-1)	$8(\frac{1}{2\sqrt{2}})$
7		3(-1)	2(-1)		6(-1)	5(-1)		$8(-\frac{1}{4})$
8	$8(\frac{1}{\sqrt{2}})$	$8(-\frac{1}{2})$	$8(-\frac{1}{2})$	$8(-\frac{1}{4})$	$8(\frac{1}{2\sqrt{2}})$	$8(\frac{1}{2\sqrt{2}})$	$8(-\frac{1}{4})$	$(c_{88}^k)^a$

$$^a c_{88}^k = 1(\frac{1}{\sqrt{2}}), 2(-\frac{1}{2}), 3(-\frac{1}{2}), 4(-\frac{1}{4}), 5(\frac{1}{2\sqrt{2}}), 6(\frac{1}{2\sqrt{2}}), 7(-\frac{1}{4}).$$

Now, it follows from Eq. (15) that the RG equations for the couplings η (instead of λ):

$$\begin{aligned} \dot{\eta}_1 &= \eta_1 + \frac{1}{2} (\eta_1 \eta_4 + \eta_2 \eta_5 + \eta_3 \eta_6) - \frac{1}{4} \eta_8^2, \\ \dot{\eta}_2 &= \eta_2 + \frac{1}{2} (2\eta_1 \eta_5 + \eta_3 \eta_7) + \frac{1}{4} \eta_8^2, \\ \dot{\eta}_3 &= \eta_3 + \frac{1}{2} (2\eta_1 \eta_6 + \eta_2 \eta_7) + \frac{1}{4} \eta_8^2; \\ \dot{\eta}_4 &= 2\eta_1^2 + \frac{1}{2} (\eta_5^2 + \eta_6^2) + \frac{1}{4} \eta_8^2, \\ \dot{\eta}_5 &= 2\eta_1 \eta_2 + \frac{1}{2} (\eta_4 \eta_5 + \eta_6 \eta_7) - \frac{1}{4} \eta_8^2, \\ \dot{\eta}_6 &= 2\eta_1 \eta_3 + \frac{1}{2} (\eta_4 \eta_6 + \eta_5 \eta_7) - \frac{1}{4} \eta_8^2, \\ \dot{\eta}_7 &= 2\eta_2 \eta_3 + \eta_5 \eta_6 + \frac{1}{4} \eta_8^2; \\ \dot{\eta}_8 &= \frac{3}{2} \eta_8 - \eta_1 \eta_8 + \frac{1}{2} (\eta_2 + \eta_3) \eta_8 \\ &\quad - \frac{1}{4} (\eta_5 + \eta_6) \eta_8 + \frac{1}{8} (\eta_4 + \eta_7) \eta_8. \end{aligned} \quad (23)$$

The perturbative central charge (16) for the present

model in terms of η is

$$\begin{aligned}
C(\{\eta\}) = & 2 - \frac{3}{4}(2\eta_1^2 + \eta_2^2 + \eta_3^2 + \frac{3}{2}\eta_8^2) \\
& - \frac{3}{2}(\eta_1\eta_2\eta_5 + \eta_1\eta_3\eta_6 + \frac{1}{2}\eta_2\eta_3\eta_7 + \frac{1}{4}\eta_5\eta_6\eta_7) \\
& - \frac{3}{16}(4\eta_1^2 + \eta_5^2 + \eta_6^2)\eta_4 \\
& + \frac{3}{8}(2\eta_1 - \eta_2 - \eta_3 - \frac{1}{4}\eta_4 \\
& + \frac{1}{2}\eta_5 + \frac{1}{2}\eta_6 - \frac{1}{4}\eta_7)\eta_8^2. \quad (24)
\end{aligned}$$

B. RG equations for model (II)

Comparing with the previous model, the only difference now is replacing \mathcal{H}_h by \mathcal{H}_Δ , i.e.,

$$\mathcal{O}_8 = 2\sigma_1\sigma_2\sigma_3\sigma_0 = 2\sin\sqrt{\pi}\Phi_+\sin\sqrt{\pi}\Phi_-, \quad (25)$$

$$\lambda_8 \equiv \frac{\eta_8}{2} = \frac{\pi\Delta}{2v}, \quad (26)$$

and Eq. (21) is modified to be

$$\begin{aligned}
\mathcal{O}_8(z, \bar{z})\mathcal{O}_8 \sim & \frac{\alpha}{|z|} + \frac{1}{\sqrt{2}}\mathcal{O}_1 + \frac{1}{2}(\mathcal{O}_2 + \mathcal{O}_3) \\
& - \left(\frac{\alpha}{|z|}\right)^{-1} \left[\frac{1}{2\sqrt{2}}(\mathcal{O}_5 + \mathcal{O}_6) + \frac{1}{4}(\mathcal{O}_4 + \mathcal{O}_7) \right], \quad (27)
\end{aligned}$$

yielding

$$\begin{aligned}
c_{88}^k = & 1\left(\frac{1}{\sqrt{2}}\right), 2\left(\frac{1}{2}\right), 3\left(\frac{1}{2}\right), \\
& 4\left(-\frac{1}{4}\right), 5\left(-\frac{1}{2\sqrt{2}}\right), 6\left(-\frac{1}{2\sqrt{2}}\right), 7\left(-\frac{1}{4}\right). \quad (28)
\end{aligned}$$

However, as we have known, the symmetry of model (II) is higher than that of model (I)—the $O(3)$ symmetry in the triplet sector [i.e., the $SU(2)$ symmetry in the original lattice model] should remain. In other words, the division of the triplet into doublet and singlet is futile in the present case. This fact is reflected in the RG equations also. From Eqs. (23), by reversing the signs of the coefficients involving c_{88}^2 , c_{88}^3 , c_{88}^5 , and c_{88}^6 , three of the eight equations are redundant, implying $\eta_1 = \eta_2$, $\eta_4 = \eta_5$, and $\eta_6 = \eta_7$. As a result, the RG equations degenerate to

$$\begin{aligned}
\dot{\eta}_1 = & \eta_1 + \frac{1}{2}(2\eta_1\eta_4 + \eta_3\eta_6) - \frac{1}{4}\eta_8^2, \\
\dot{\eta}_3 = & \eta_3 + \frac{3}{2}\eta_1\eta_6 - \frac{1}{4}\eta_8^2; \\
\dot{\eta}_4 = & 2\eta_1^2 + \frac{1}{2}(\eta_4^2 + \eta_6^2) + \frac{1}{4}\eta_8^2, \\
\dot{\eta}_6 = & 2\eta_1\eta_3 + \eta_4\eta_6 + \frac{1}{4}\eta_8^2; \\
\dot{\eta}_8 = & \frac{3}{2}\eta_8 - \frac{1}{2}(3\eta_1 + \eta_3)\eta_8 + \frac{3}{8}(\eta_4 + \eta_6)\eta_8, \quad (29)
\end{aligned}$$

and the central charge to

$$\begin{aligned}
C(\{\eta\}) = & 2 - \frac{3}{4}(3\eta_1^2 + \eta_3^2 + \frac{3}{2}\eta_8^2) \\
& - \frac{3}{2}(\eta_1^2\eta_4 + \frac{3}{2}\eta_1\eta_3\eta_6 + \frac{1}{4}\eta_4\eta_6^2) \\
& - \frac{3}{16}(4\eta_1^2 + \eta_4^2 + \eta_6^2)\eta_4 \\
& + \frac{3}{8}(3\eta_1 + \eta_3 - \frac{3}{4}\eta_4 - \frac{3}{4}\eta_6)\eta_8^2. \quad (30)
\end{aligned}$$

IV. SOLUTIONS TO THE RG EQUATIONS AND THE EMERGING PHASE DIAGRAMS

To analyze the infrared behaviors of our present models, in this section, we numerically integrate these two sets of RG Eqs. (23) and (29) to depict generic phase diagrams for the spin ladder under a staggered field or dimerization. On account of the fact that for a system in a massive regime, the role of marginal coupling is usually exhausted by renormalizing the mass and velocity, it is reasonable to take no thought of these marginal perturbations at the outset and argue that the overall qualitative feature remains correct although the position and shape of phase boundary may not be exact. Let us begin with a known system—the generalized spin ladder (1)⁹—as an example. A variant of this model includes four-spin ring exchange, which is believed to be relevant to some exotic properties in real ladder materials.^{16,17,18}

In the following we denote the bare ultraviolet couplings by $\eta^{(0)} \equiv \eta(L=1)$ and the renormalized infrared couplings by $\eta^{(\infty)} \equiv \eta(L=\infty)$.

A. Phase diagram of the generalized spin ladder

In this case, the RG equations are trivially $\dot{\eta}_1 = \eta_1$ and $\dot{\eta}_3 = \eta_3$. Unless the initial value (bare coupling) vanishes, $\eta_1^{(0)} = 0$ or $\eta_3^{(0)} = 0$, the system is always renormalized to some strong-coupling massive phase as $L \rightarrow \infty$. Because of relations in Eqs. (20), $\eta_1^{(0)} = \frac{m_t\alpha}{v}$ and $\eta_3^{(0)} = \frac{m_s\alpha}{v}$, we conclude that $m_t = 0$ and $m_s = 0$ are phase transition lines on which the model becomes critical. They belong to the universality classes of critical $SU(2)_2$ WZNW model and Z_2 Ising model, respectively.⁹ As a base for our further exploration, we draw the phase diagram of the generalized spin ladder (1) in Fig. 1.

According to Ref. 9, there are four massive phases divided by two critical lines. The second and fourth quadrants of the figure are two Haldane (H^\pm) spin liquid phases, and the first and third quadrants belong to spontaneously dimerized (sD^\pm) phases. The “+/-” sectors are actually related by duality of reversing the signs of the masses. The axis of abscissas represents a critical model with an $SU(2)_2$ WZNW universality class (L: $SU(2)_2$), and the axis of ordinates a Z_2 (Ising) one (L: Z_2). Although the Haldane phases and the dimer phases share

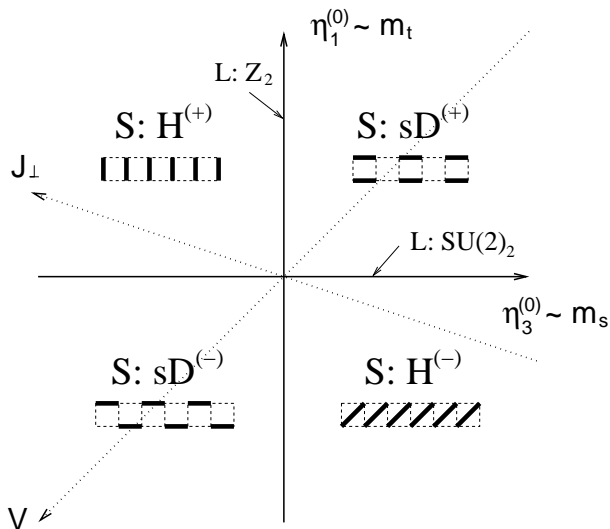


FIG. 1: Phase diagram of the generalized spin ladder. There exist two critical lines L: $SU(2)_2$ and L: Z_2 , and four massive sheets S: $H^{(\pm)}$ and S: $sD^{(\pm)}$. Notice the dimers in the Haldane phases are only symbolic rather than a true order.

the feature of non-vanishing topological string order parameter in common and thermodynamically they are indistinguishable, the symmetry of the ground state and the behavior of the dynamical susceptibility are completely different.

(i) S: $H^{(+)}$ phase [$\eta_1^{(\infty)} = +\infty$, $\eta_3^{(\infty)} = -\infty$]: Neither parity (site or bond) symmetry nor translational symmetry is broken. There is a coherent peak for the dynamical spin susceptibility at $q_{\perp} = \pi$, $q \sim \pi$, $\omega \sim |m_t|$, characterizing coherent $S = 1$ single-magnon excitations.

(ii) S: $H^{(-)}$ phase [$\eta_1^{(\infty)} = -\infty$, $\eta_3^{(\infty)} = +\infty$]: No symmetry breaking (except for the hidden string order). The peak is at $q_{\perp} = 0$, $q \sim \pi$, $\omega \sim |m_t|$ instead.

(iii) S: $sD^{(+)}$ phase [$\eta_1^{(\infty)} = +\infty$, $\eta_3^{(\infty)} = +\infty$]: The discrete site-parity and translational symmetries are spontaneously broken. The corresponding order parameter is $\langle (-1)^n (\mathbf{S}_{1,n} \cdot \mathbf{S}_{1,n+1} + \mathbf{S}_{2,n} \cdot \mathbf{S}_{2,n+1}) \rangle \neq 0$ (0-phase). No coherent peak in the spin susceptibility (square-root singularity only).

(iv) S: $sD^{(-)}$ phase [$\eta_1^{(\infty)} = -\infty$, $\eta_3^{(\infty)} = -\infty$]: The discrete symmetries are broken with an order parameter $\langle (-1)^n (\mathbf{S}_{1,n} \cdot \mathbf{S}_{1,n+1} - \mathbf{S}_{2,n} \cdot \mathbf{S}_{2,n+1}) \rangle \neq 0$ (π -phase). No coherent peak either.

We also show in the figure the directions of the lattice model parameters J_{\perp} and V via relation (8), although the exact scales for the coordinates are not known. We find that the standard ladder with positive, antiferro-(negative, ferro-) J_{\perp} is in Haldane $H^{(+)}$ ($H^{(-)}$) phase. The pure four-spin coupling model with $J_{\perp} = 0$ is in the $sD^{(-)}$ phase when $V > 0$ or in the $sD^{(+)}$ phase when $V < 0$. This is a special case with a higher symmetry.

It is also interesting to check in RG sense the flow of

the central charge. For this simple model we have

$$C = 2 - \frac{3}{4}(3\eta_1^2 + \eta_3^2). \quad (31)$$

Considering this is a perturbative one-loop result and should not be taken seriously when η approaches unity, we assume that we can mimic the true fixed point property by introducing a cut-off in η . If we are allowed to choose this cut-off to be $\sqrt{\frac{2}{3}}$, the correct central charges for both $SU(2)_2$ and Z_2 can be recovered, since for the former when $(\eta_1^*, \eta_3^*) = (0, \sqrt{\frac{2}{3}})$, $C^* = \frac{3}{2}$, and for the latter when $(\eta_1^*, \eta_3^*) = (\sqrt{\frac{2}{3}}, 0)$, $C^* = \frac{1}{2}$. The existence of the $SU(2)_2$ criticality was recently confirmed by a direct estimate of the numerical value of the central charge.¹⁷

B. Phase diagram of model (I)

Model (I) is the generalized spin ladder (1) in a staggered field (2). The RG equations regarding the relevant perturbations now become

$$\begin{aligned} \dot{\eta}_1 &= \eta_1 - \frac{1}{4}\eta_8^2, \\ \dot{\eta}_2 &= \eta_2 + \frac{1}{4}\eta_8^2, \\ \dot{\eta}_3 &= \eta_3 + \frac{1}{4}\eta_8^2, \\ \dot{\eta}_8 &= \frac{3}{2}\eta_8 - \eta_1\eta_8 + \frac{1}{2}(\eta_2 + \eta_3)\eta_8. \end{aligned} \quad (32)$$

Evidently, the equations are invariant under the transformation $\eta_8 \rightarrow -\eta_8$, which corresponds to $h \rightarrow -h$ in the original spin model. We need only deal with the positive case. At first glance the system has two mathematical fixed points: (a) $(\eta_1^*, \eta_2^*, \eta_3^*, \eta_8^*) = (0, 0, 0, 0)$ and (b) $(\frac{3}{4}, -\frac{3}{4}, -\frac{3}{4}, \sqrt{3})$. The one at the origin is an unstable fixed point recounting two decoupled chains as our starting point; while the fixed point (b) is fallacious. This is due to the fact that η_1 and η_2 are not completely independent, i.e., initially $\eta_1^{(0)} = \eta_2^{(0)} = \frac{m_t \alpha}{v}$, rendering the fixed point (b) physically inaccessible. However, the values in (b) do have full play in the the structure of the phase diagram.

The emerging phase diagram of model (I) is shown in Fig. 2. It is notable that all the interesting phases lie in the first three quadrants of the base and the fourth quadrant is in some sense rather barren. This is controlled by the “fixed point” (b) mentioned above. To make the structure clearer, we anatomically plot figures in two intersecting planes (see Fig. 3). Various phases are labeled in the figures, where “B” denotes a block or bulk space that is always massive, “S” stands for a surface or sheet as phase boundary separating two different phases, which can be critical or first-ordered, and “L” is an intersectional line of two sheets.

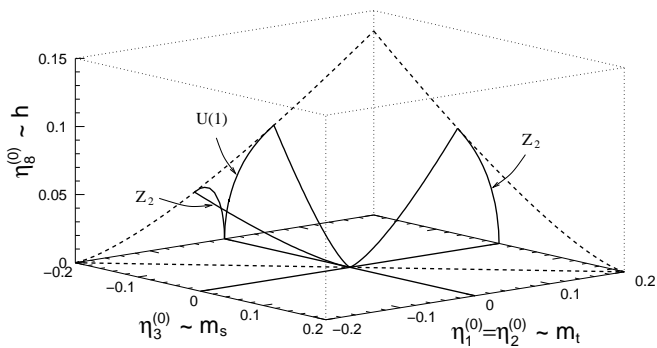


FIG. 2: Phase diagram of the generalized spin ladder in a staggered field. The massive phases occupying different blocks are separated by interfaces either second-ordered (enclosed by solid line) or with the transition nature unknown from the RG equations alone (dashed line).

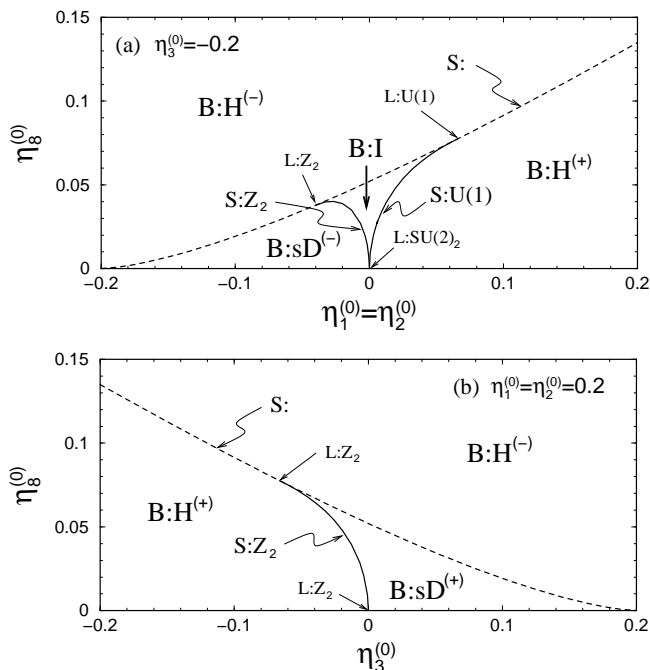


FIG. 3: Sectional plot of the phase diagram of the generalized spin ladder in a staggered field: (a) $\eta_3^{(0)}$ is a constant as -0.2 . (b) $\eta_1^{(0)} = \eta_2^{(0)}$ is a constant as 0.2 .

Now let us interpret in some detail the obtained phase diagram. We take the example with a parameter range where two consecutive phase transitions occur when increasing the staggered field—one belongs to the U(1) universality class; the other's property is not determined by the RG theory itself (probably first-ordered). Suppose a generalized spin ladder offers such a kind of parameters:

$$\begin{aligned} m_t &\sim \eta_1^{(0)} = \eta_2^{(0)} = 0.01, \\ m_s &\sim \eta_3^{(0)} = -0.2, \end{aligned} \quad (33)$$

where $\eta^{(0)}$'s are bare-couplings as the initial values of the differential equations (32): $\eta^{(0)} \equiv \eta(L=1)$.

Now the system is subjected to a staggered field. It is found when the field is increased to

$$h_{c1} \sim (\eta_8^{(0)})_{c1} = 0.0354863, \quad (34)$$

the system undergoes a second-order phase transition with a U(1) universality class (or Gaussian fixed point). The behaviors of the RG flows in the vicinity of this transition is shown in Figs. 4 (a), (b), and (c). Below

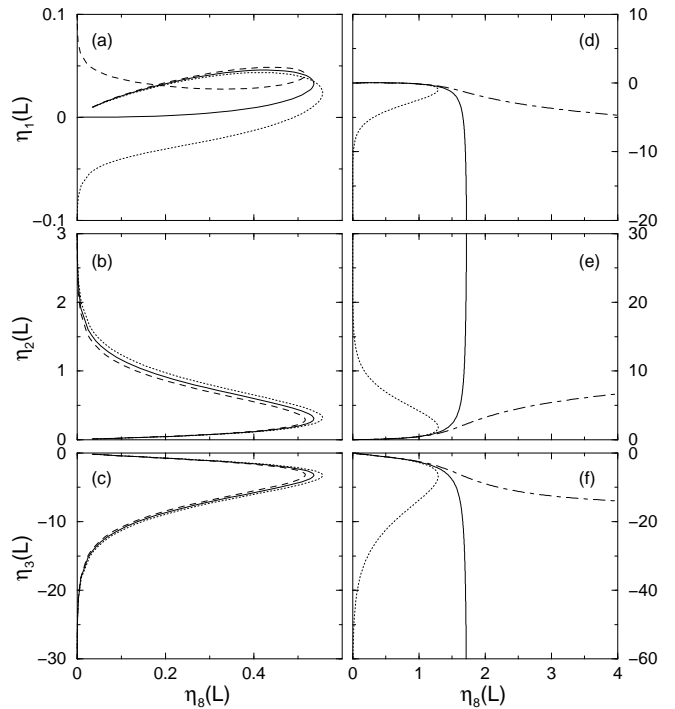


FIG. 4: Parametric plot of the RG flows across two phase transitions. The figures in the left column describe the flows in the vicinity of the U(1) transition, where the solid lines correspond to $\eta_8^{(0)} = (\eta_8^{(0)})_{c1}$, the dashed lines to $\eta_8^{(0)} = (\eta_8^{(0)})_{c1} - 0.001$, and the dotted lines to $\eta_8^{(0)} = (\eta_8^{(0)})_{c1} + 0.001$. The figures in the right column are in the vicinity of the second (unidentified) transition, where the solid lines correspond to $\eta_8^{(0)} = (\eta_8^{(0)})_{c2}$, the dotted lines to $\eta_8^{(0)} = (\eta_8^{(0)})_{c2} - 0.001$, and the dash-dotted lines to $\eta_8^{(0)} = (\eta_8^{(0)})_{c2} + 0.001$. Notice in panel (f) the dash-dotted line for $\eta_3(L)$ eventually approaches $+\infty$ after an upturn that is not shown in the figure.

the U(1) transition the system is in the bulk massive phase B: H⁽⁺⁾ characterized by the couplings renormalized to $(\eta_1^{(\infty)}, \eta_2^{(\infty)}, \eta_3^{(\infty)}, \eta_8^{(\infty)}) = (+\infty, +\infty, -\infty, 0)$ (the dashed lines in the figures). At the transition, the infrared property becomes $(\eta_1^{(\infty)}, \eta_2^{(\infty)}, \eta_3^{(\infty)}, \eta_8^{(\infty)}) = (0, +\infty, -\infty, 0)$ (the solid lines in the figures). Since η_1 is proportional to the split doublet mass, m_t^d , it is bound to attribute this transition to a U(1) character. Now we are in the bulk phase of B: I characterized by $(-\infty, +\infty, -\infty, 0)$ (the dotted lines in the figures). This

is an intermediate phase interpolating between the Haldane phase and the spontaneously dimered phase. The most distinctive features of this phase are that it has only transverse coherent spin excitations and longitudinal string order parameter. (For detailed properties, cf. Ref. 8.)

If the staggered field is further increased to reach the point

$$h_{c2} \sim (\eta_8^{(0)})_{c2} = 0.0560487, \quad (35)$$

the second transition occurs. The RG flows around this transition is shown in Figs. 4 (d), (e), and (f). At the transition the couplings are renormalized to $(-\infty, +\infty, -\infty, \sqrt{3})$ (the solid lines in the figures). After the transition the system enters the B: $H^{(-)}$ phase characterized by $(-\infty, +\infty, +\infty, \infty)$ (the dash-dotted lines in the figures). Unfortunately, we can tell very little from the present scheme regarding the property of this transition. It may be a first-order transition or even a crossover.

In this way, we are able to classify most of the phases and transitions by the infrared properties inferred from the RG equations. We summarize the main results as follows.

a. Bulks :

	$\eta_1^{(\infty)}$	$\eta_2^{(\infty)}$	$\eta_3^{(\infty)}$	$\eta_8^{(\infty)}$
B:sD ⁽⁺⁾	$+\infty$	$+\infty$	$+\infty$	0
B:sD ⁽⁻⁾	$-\infty$	$-\infty$	$-\infty$	0
B:H ⁽⁺⁾	$+\infty$	$+\infty$	$-\infty$	0
B:H ⁽⁻⁾	$-\infty$	$+\infty$	$+\infty$	∞
B:I	$-\infty$	$+\infty$	$-\infty$	0

(36)

Comparing with the zero-field case (previous subsection), we find that three massive phases sD^(±) and H⁽⁺⁾ are essentially passed from their $h = 0$ counterparts directly except for the broken symmetry $\eta_1 \neq \eta_2$. However, B: H⁽⁻⁾ phase is different from S: H⁽⁻⁾ in the sense that $\eta_2^{(\infty)} \rightarrow +\infty$ instead of $-\infty$ and $\eta_8^{(\infty)} \rightarrow \infty$ instead of 0. Obviously, B: I is a totally new phase which has no zero-field counterpart.

b. Sheets :

	$\eta_1^{(\infty)}$	$\eta_2^{(\infty)}$	$\eta_3^{(\infty)}$	$\eta_8^{(\infty)}$
S:U(1) [H ⁽⁺⁾ -I]	0	$+\infty$	$-\infty$	0
S:Z ₂ [sD ⁽⁻⁾ -I]	$-\infty$	0	$-\infty$	0
S:Z ₂ [H ⁽⁺⁾ -sD ⁽⁺⁾]	$+\infty$	$+\infty$	0	0
S:Z ₂ [sD ⁽⁻⁾ -H ⁽⁻⁾]	$-\infty$	$-\infty$	$-\infty$	$\sqrt{3}$
S: [I-H ⁽⁻⁾]	$-\infty$	$+\infty$	$-\infty$	$\sqrt{3}$
S: [H ⁽⁺⁾ -H ⁽⁻⁾]	$+\infty$	$+\infty$	$-\infty$	$\sqrt{3}$
S: [sD ⁽⁺⁾ -H ⁽⁻⁾]	$+\infty$	$+\infty$	$+\infty$	$\sqrt{3}$

(37)

It is perspicuous that the critical surfaces split from the SU(2)₂ critical line and having U(1) and Z₂ criticalities correspond to the infrared fixed points with $(\eta_1, \eta_8) \propto (m_t^d, h) \rightarrow (0, 0)$ and $(\eta_2, \eta_8) \propto (m_t^s, h) \rightarrow (0, 0)$, respectively. The other Z₂ criticality is trivially same as and

connected to the one when $h = 0$, $(\eta_3, \eta_8) \propto (m_s, h) \rightarrow (0, 0)$. At least one of the four unknown boundaries (dashed lines in Fig. 2 and 3) can be identified as Z₂, i.e., S: [sD⁽⁻⁾-H⁽⁻⁾]. The reason is to be shown soon.

c. Lines :

	$\eta_1^{(\infty)}$	$\eta_2^{(\infty)}$	$\eta_3^{(\infty)}$	$\eta_8^{(\infty)}$
L:U(1) [H ⁽⁺⁾ -I-H ⁽⁻⁾]	$+\frac{3}{4}$	$+\infty$	$-\infty$	$\sqrt{3}$
L:Z ₂ [sD ⁽⁻⁾ -I-H ⁽⁻⁾]	$-\infty$	$-\frac{3}{4}$	$-\infty$	$\sqrt{3}$
L:Z ₂ [H ⁽⁺⁾ -sD ⁽⁺⁾ -H ⁽⁻⁾]	$+\infty$	$+\infty$	$-\frac{3}{4}$	$\sqrt{3}$

(38)

These lines are intersections of two surfaces. The special values here are associated with the “fixed point” (b) of Eqs. (32).

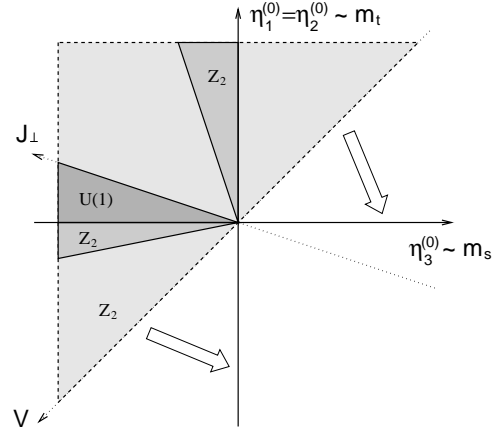


FIG. 5: A top-view plot of the phase diagram of the generalized spin ladder in a staggered field. The true phase boundaries in the base ($h = 0$) should be extended as shown by the arrows.

To close our discussion, we show in Fig. 5 a top-view of the phase diagram. The U(1) zone is confined in a wedged area demarcated by the SU(2)₂ line $\eta_1^{(0)} = \eta_2^{(0)} = 0$ and $\eta_1^{(0)} = \eta_2^{(0)} = -\frac{1}{3}\eta_3^{(0)} > 0$, i.e., $m_t = -\frac{1}{3}m_s > 0$. The latter condition amounts to $V = 0$ and $J_\perp > 0$ via relation (8), coinciding with the location of a standard spin ladder with antiferromagnetic interchain coupling. The adjacent Z₂ region is delimited by condition $\eta_1^{(0)} = \eta_2^{(0)} = \frac{1}{5}\eta_3^{(0)} < 0$. The trivial Z₂ region is within the Z₂ line $\eta_3^{(0)} = 0$ and $\eta_1^{(0)} = \eta_2^{(0)} = -3\eta_3^{(0)} > 0$. The unidentified sheet have $\eta_1^{(0)} = \eta_2^{(0)} = \eta_3^{(0)}$ as its boundary in the base. This is a model with $J_\perp = 0$, i.e., only four-spin interchain coupling. However, one might have noticed that there is something unnatural here. Considering the internal relation between the B: H⁽⁻⁾ phase in the bulk and the S: H⁽⁻⁾ phase in the base, we suggest in the true situation the boundary of this sheet should bend over to connect to the critical lines in the base (as shown by the arrows in Fig. 5). By combining the “integrating out” method and the study of the bosonized model, we observe that a Z₂ surface, connecting two axes, covers the whole third quadrant in Fig. 5.

C. Phase diagram of model (II)

Now we turn to Model (II), the generalized spin ladder (1) under dimerization (3). It follows from Eqs. (29) by retaining only the relevant couplings:

$$\begin{aligned}\dot{\eta}_1 &= \eta_1 - \frac{1}{4}\eta_8^2, \\ \dot{\eta}_3 &= \eta_3 - \frac{1}{4}\eta_8^2, \\ \dot{\eta}_8 &= \frac{3}{2}\eta_8 - \frac{1}{2}(3\eta_1 + \eta_3)\eta_8.\end{aligned}\quad (39)$$

This is a model with an unbroken $O(3)$ symmetry. As before, we have an invariance $\eta_8 \rightarrow -\eta_8$ (i.e., $\Delta \rightarrow -\Delta$). In contrast with the previous model, now the system has really a fixed point $(\eta_1^*, \eta_3^*, \eta_8^*) = (\frac{3}{4}, \frac{3}{4}, \sqrt{3})$ besides the trivial one at the origin. This fixed point occurs at $\eta_1 = \eta_3$, or equivalently $m_t = m_s$, corresponding to the pure four-spin coupling model ($J_{\perp} = 0$) when the system has a higher $SU(2) \times SU(2) \approx O(4)$ symmetry. This is also the condition for the line where the $SU(2)_1$ sheet merges the Z_2 sheet into the $SU(2)_2$ sheet. The RG flows around this fix point are shown in Fig. 6, where we choose the

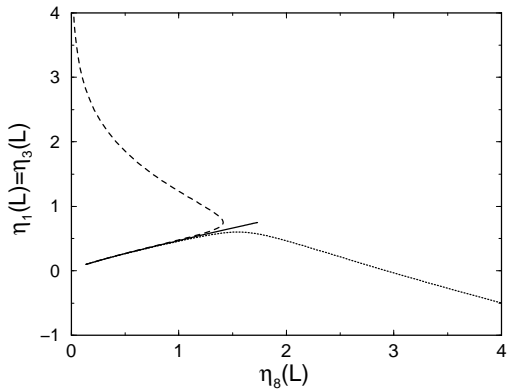


FIG. 6: RG flows to the fixed point $(\eta_1^*, \eta_3^*, \eta_8^*) = (\frac{3}{4}, \frac{3}{4}, \sqrt{3})$ (solid line) at $\eta_1^{(0)} = \eta_3^{(0)} = 0.1$ and $(\eta_8^{(0)})_c = 0.137410$, and below $(\eta_8^{(0)} = (\eta_8^{(0)})_c - 0.001$, dashed line) and above $(\eta_8^{(0)} = (\eta_8^{(0)})_c + 0.001$, dotted line) the transition.

initial values for the base quantities: $\eta_1^{(0)} = \eta_3^{(0)} = 0.1$. The initial value of the dimerization for the fixed point is $(\eta_8^{(0)})_c = 0.137410$.

The phase diagram of this model is plotted in Fig. 7, and Fig. 8 is for the sectional pictures of the same phase diagram, where we have labeled various phases. As before, the classification of phases and criticalities is associated with the infrared properties of the system resulted from the RG equations.

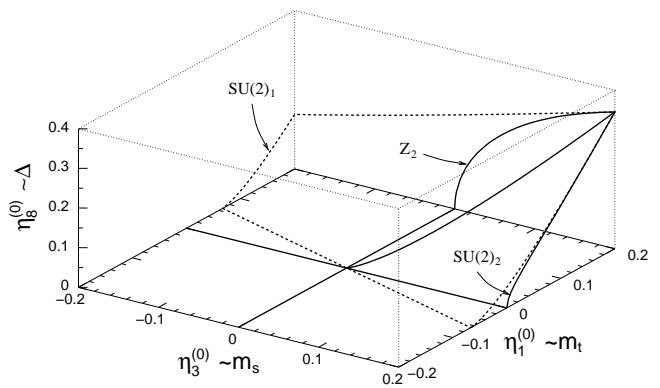


FIG. 7: Phase diagram of the generalized spin ladder under π -phase dimerization.

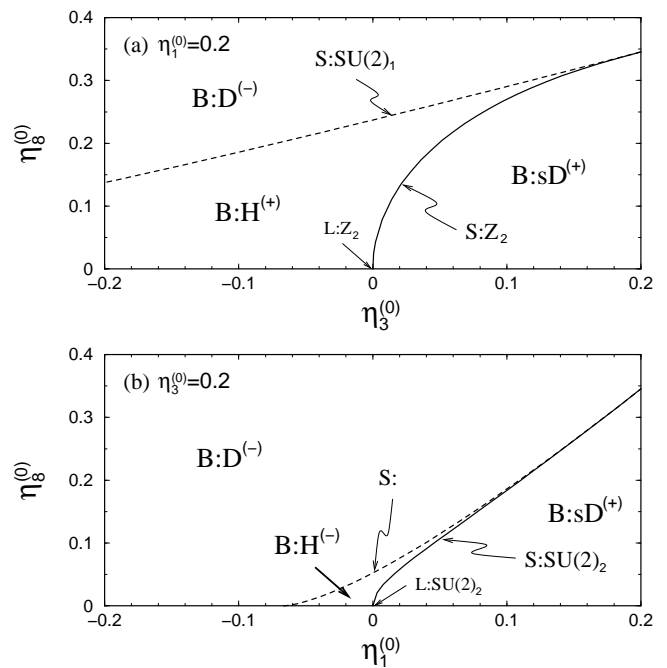


FIG. 8: Sectional plot of the phase diagram of the generalized spin ladder under dimerization.

a. *Bulks* :

	$\eta_1^{(\infty)}$	$\eta_3^{(\infty)}$	$\eta_8^{(\infty)}$
B:H ⁽⁺⁾	$+\infty$	$-\infty$	0
B:H ⁽⁻⁾	$-\infty$	$+\infty$	0
B:sD ⁽⁺⁾	$+\infty$	$+\infty$	0
B:D ⁽⁻⁾	$-\infty$	$-\infty$	∞

(40)

Three massive phases H^{\pm} and $sD^{(+)}$ are same as their $\Delta = 0$ counterparts. Since the symmetry of phase $sD^{(+)}$ is different from the explicit dimerization perturbation (3), it is still spontaneously dimerized. However, B: $D^{(-)}$ phase is different from S: $sD^{(-)}$, because now the system is explicitly dimerized with the same symmetry of the

perturbed Hamiltonian. In the infrared limit $\eta_8^{(\infty)} \rightarrow \infty$ instead of 0. It is also noticed from the figures that phase B: $H^{(-)}$ is restricted to a rather small region in the phase space. This may not be the real situation (see discussions at the end of this section).

b. Sheets :

	$\eta_1^{(\infty)}$	$\eta_3^{(\infty)}$	$\eta_8^{(\infty)}$
S:SU(2) ₂ [sD ⁽⁺⁾ -H ⁽⁻⁾]	0	$+\infty$	0
S:Z ₂ [sD ⁽⁺⁾ -H ⁽⁺⁾]	$+\infty$	0	0
S:SU(2) ₁ [H ⁽⁺⁾ -D ⁽⁻⁾]	$+\infty$	$-\infty$	$\sqrt{3}$
S: [H ⁽⁻⁾ -D ⁽⁻⁾]	$-\infty$	$+\infty$	$\sqrt{3}$

(41)

Like the case before, the identification of the SU(2)₂ and Z₂ criticalities is directly due to the fact that in addition to the dimerization ($\eta_8^{(\infty)}$), the triplet ($\eta_1^{(\infty)}$) and singlet ($\eta_3^{(\infty)}$) masses are renormalized to vanish, respectively. However, the reference of the interface between phases H⁽⁺⁾ and D⁽⁻⁾ to an SU(2)₁ criticality is a bit subtle. This conclusion is drawn from other studies of the standard ladder under dimerization.^{7,19,20,21} In Ref. 19, a standard spin- $\frac{1}{2}$ ladder with ferromagnetic interchain coupling under 0-phase dimerization (the dual case of our present model) was semiclassically mapped onto an O(3) nonlinear sigma model with some topological angle. The SU(2)₁ criticality is realized when this angle equals π . On the other hand, an effective Hamiltonian was explicitly derived in Ref. 7 which describes the same transition in terms of a single spin- $\frac{1}{2}$ chain with bond alternation, and the transmutation of all physical quantities from the ultraviolet fixed point to the infrared fixed point was established. We have only one unidentified surface, S: [H⁽⁻⁾-D⁽⁻⁾], in this model.

c. Line :

	$\eta_1^{(\infty)}$	$\eta_3^{(\infty)}$	$\eta_8^{(\infty)}$
L:SU(2) ₂ [sD ⁽⁺⁾ -H ⁽⁺⁾ -D ⁽⁻⁾ -H ⁽⁻⁾]	$\frac{3}{4}$	$\frac{3}{4}$	$\sqrt{3}$

(42)

The only critical line in this model represents the fixed point of Eqs. (39), the RG flow for the point on which is shown in Fig. 6. This is a very special line with a higher O(4) symmetry: it is not only the ridge line where all sheets meet, but also the common boundary shared by all four phases (blocks) of the model.

Since the obtained phase diagram is grounded on the relevant part of the one-loop RG equations, the position of the phase boundaries may not be so correct. For instance, considering the intimacy between the bulk B: D⁽⁻⁾ phase and the S: sD⁽⁻⁾ phase in the base, most plausibly the SU(2)₁ sheet is connected to the SU(2)₂ line of $\Delta = 0$, and the boundary for the unidentified sheet is pushed to connect to the Z₂ line in the base (see Fig. 9). So the space for the bulk B: H⁽⁻⁾ phase is considerably enlarged. This is supported by the fact that, as we have mentioned, the ($J_{\perp} > 0$) standard ladder ($V = 0$) undergoes the SU(2)₁ transition under the (π -phase) dimerization. So the SU(2)₁ sheet cannot terminate at the loca-

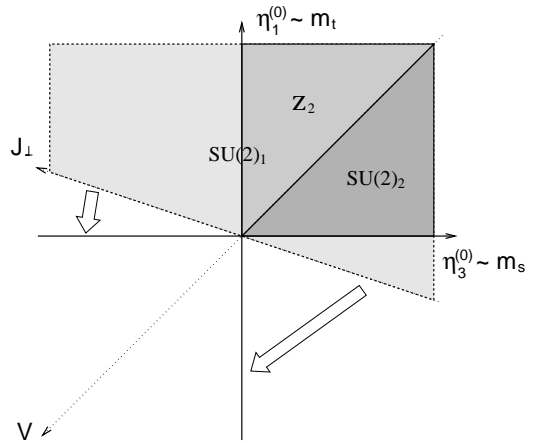


FIG. 9: Top-view plot of the phase diagram of the generalized spin ladder under dimerization. The true SU(2)₁ sheet should connect to the SU(2)₂ line in the base, and the unidentified sheet to the Z₂ line in the base (as shown by the arrows).

tion which is a result from the approximate RG Eqs. (39) as shown in Fig. 7.

V. SUMMARY AND DISCUSSIONS

Based on the one-loop RG equations and the assumption that the relevant perturbations govern the relative structure of various phases in the parameter space, we have speculated from the infrared properties of these equations the phase diagrams of two related spin ladder models in the weak-coupling regime.

In model (I), the external staggered field breaks the SU(2) symmetry down to U(1) and Z₂, so that the criticalities at most have the same symmetries and no room for SU(2) to live. Indeed, we find both U(1) and Z₂ criticalities come forth with the introduction of the staggered field (see Fig. 2 and 5), which actually evolve from the underlying SU(2)₂ criticality in absence of the field. The present result confirms the picture we obtained through a somewhat different approach in Ref. 8. In that study, we literally integrated out the fast degrees of freedom associated with the singlet modes close to the SU(2)₂ line and derived an effective action which describes the triplet sector with anisotropy induced by the staggered field. The vanishing of the split effective triplet mass manifests the criticality accordingly. The new observation is that the intermediate phase (B: I), which interpolates between the Haldane phase (B: H⁽⁺⁾) and the dimer phase (B: sD⁽⁻⁾), is restricted to a very limited region, and there should exist another (unidentified) transition which separates B: I phase from the large- h (Haldane) phase (B: H⁽⁻⁾) which occupies most of the space in the phase diagram. From the infrared property (36), we see that B: I phase is quite unique entirely due to the staggered field, and there is no resemblance preexisting when $h = 0$.

Comparing with model (I), model (II) is relatively sim-

ple in the sense that the $SU(2)$ symmetry is unbroken and the $O(3)$ symmetry in the triplet sector remains, and the number of RG equations is thus reduced. All four bulk phases can basically be traced back to their counterparts when $\Delta = 0$. None the less, as we have seen, the phase diagram of this model is by no means uneventful (see Fig. 7 and 9). The phenomenon extremely intriguing is the merging of $SU(2)_1$ and Z_2 critical sheets into $SU(2)_2$ sheet. The information encoded in the RG equations reveals that this occurs at some critical dimerization strength $\Delta_c(V)$ when the system has a higher $O(4)$ symmetry or $SU(2) \times SU(2)$ in the original lattice model, i.e., $J_\perp = 0$. The merging line with $SU(2)_2$ criticality is shared by all four massive phases of the model.

The benevolent aspect of our present theory is that we are able to assort different phases according to their infrared properties from the RG flows, and the identification of the critical sheets that emerge from the underlying critical lines in the base should be reliable. These critical sheets, including two Z_2 and $U(1)$ in model (I) and $SU(2)_2$ and Z_2 in model (II), can also be verified to exist²² by means of “integrating out” procedure employed in Ref. 8, although the terminating positions of these sheets are unknown by this approach. However, as one may have perceived, the insolvency of the present

theory is that not all of the transitions can be attributed. Even worse is the phase boundaries resolved from the one-loop equations may not be accurate. (See our suggestions for the modification of the phase diagrams in Fig. 5 and 9.) Therefore, although the topology of the phase diagrams we believe has been overall and qualitatively captured, the unwavering pin-pointing of the phase diagrams has to resort to other, say numerical, methods. For example, it is predicted here for model (II) of pure four-spin interaction (V), when increasing the dimerization, there is only one second-order ($SU(2)_2$) transition which connects directly two dimerized phases with mutually mismatched orders. If adding a bit positive J_\perp coupling, one would expect two consecutive transitions: Z_2 and $SU(2)_1$ in a row.

Acknowledgments

It is a pleasure to acknowledge the helpful discussions with P. Fulde, K. Penc, R. Narayanan, T. Vekua, and M. Nakamura. Special thanks are due to A. Nersesyan for calling the problem to my attention. This work was supported under the visitors program of MPI-PKS.

-
- ¹ See, for a concise review on conformal field theory, P. Ginsparg, in *Fields, Strings and Critical Phenomena*, ed. by E. Brézin and J. Zinn-Justin (Elsevier Science, Amsterdam, 1989).
- ² See, for a review on spin chains, I. Affleck, in Ref. 1; J. Phys.: Condens. Matter **1**, 3047 (1989).
- ³ See, for a recent book on bosonization, A.O. Gogolin, A.A. Nersesyan, and A.M. Tsvelik, *Bosonization and Strongly Correlated Systems* (Cambridge University Press, Cambridge, England, 1999).
- ⁴ See, e.g., M.A. Continentino, *Quantum Scaling in Many Body Systems* (World Scientific, Singapore, 2001).
- ⁵ G. Delfino and G. Mussardo, Nucl. Phys. B **516**, 675 (1998).
- ⁶ M. Fabrizio, A.O. Gogolin, and A.A. Nersesyan, Phys. Rev. Lett. **83**, 2014 (1999); Nucl. Phys. B **580**, 647 (2000).
- ⁷ Y.-J. Wang and A.A. Nersesyan, Nucl. Phys. B **583**, 671 (2000).
- ⁸ Y.-J. Wang, F.H.L. Essler, M. Fabrizio, and A.A. Nersesyan, Phys. Rev. B **66**, 024412 (2002).
- ⁹ A.A. Nersesyan and A.M. Tsvelik, Phys. Rev. Lett. **78**, 3939 (1997).
- ¹⁰ A.K. Kolezhuk and H.-J. Mikeska, Phys. Rev. Lett. **80**, 2709 (1998).
- ¹¹ D.G. Shelton, A.A. Nersesyan, and A.M. Tsvelik, Phys. Rev. B **53**, 8521 (1996).
- ¹² Rigorously speaking, the interchain coupling J_\perp shifts the triplet and singlet velocities differently. However, we neglect this difference under the condition (4).
- ¹³ See, e.g., J.L. Cardy, in Ref. 1; A.W.W. Ludwig and J.L. Cardy, Nucl. Phys. B **285**, 687 (1987).
- ¹⁴ A.B. Zamolodchikov, JETP Lett. **43**, 730 (1986) [Pis'ma Zh. Eksp. Teor. Fiz. **43**, 565 (1986)].
- ¹⁵ The definitions and conventions we take may be found, e.g., in Appendix A of Ref. 8.
- ¹⁶ S. Brehmer, H.-J. Mikeska, M. Müller, N. Nagaosa, and S. Uchida, Phys. Rev. B **60**, 329 (1999); M. Matsuda, K. Katsumata, R.S. Eccleston, S. Brehmer, and H.-J. Mikeska, *ibid.* **62**, 8903 (2000); T.S. Nunner, P. Brune, T. Kopp, M. Windt, and M. Grüninger, *ibid.* **66**, 180404(R) (2002);
- ¹⁷ K. Hijii and K. Nomura, Phys. Rev. B **65**, 104413 (2002).
- ¹⁸ M. Müller, T. Vekua, H.-J. Mikeska, Phys. Rev. B **66**, 134423 (2002); T. Hikihara, T. Momoi, and X. Hu, Phys. Rev. Lett. **90**, 087204 (2003); A. Läuchli, G. Schmid, and M. Troyer, Phys. Rev. B **67**, 100409(R) (2003).
- ¹⁹ K. Totsuka and M. Suzuki, J. Phys.: Condens. Matter **7**, 6079 (1995).
- ²⁰ M.A. Martin-Delgado, R. Shankar, and G. Sierra, Phys. Rev. Lett. **77**, 3443 (1996); M.A. Martin-Delgado, J. Dukelsky, and G. Sierra, Phys. Lett. **250A**, 430 (1998).
- ²¹ D.C. Cabra and M.D. Grynberg, Phys. Rev. Lett. **82**, 1768 (1999).
- ²² A.A. Nersesyan and Y.-J. Wang, unpublished.